

**Technical evaluation of the Fuji
Amulet f/s Digital Breast Imaging
System
NHSBSP Equipment Report 1304**

May 2013

Authors

J M Oduko
K C Young
L Warren

National Coordinating Centre for the Physics of Mammography

Editor

Kiera Chapman
NHS Cancer Screening Programmes

Typesetting and Design

Mary Greateorex
NHS Cancer Screening Programmes

Published by

NHS Cancer Screening Programmes
Fulwood House
Old Fulwood Road
Sheffield
S10 3TH

Tel: 0114 271 1060
Fax: 0114 271 1089

Email: info@cancerscreening.nhs.uk
Website: www.cancerscreening.nhs.uk

About the NHS Cancer Screening Programmes

The NHS Cancer Screening Programmes are operated by Public Health England. Public Health England works with national and local government, industry, and the NHS to protect and improve the nation's health and support healthier choices. We address inequalities by focusing on removing barriers to good health.

We were established on 1 April 2013 to bring together public health specialists from more than 70 organisations into a single public health service.

© Crown Copyright 2013

PHE gateway number: *Pending*

Document Information	
Title	Technical evaluation of the Fuji Amulet f/s Digital Breast Imaging System
Policy/document type	NHSBSP Equipment Report
Electronic publication date	May 2013
Version	1
Superseded publications	None
Review date	None
Author/s	J M Oduko, K C Young, L Warren
Owner	May be sent to Jenny Oduko, jenny.oduko@nhs.net in readiness for review.
Document objective (clinical/healthcare/social questions covered)	Produced on behalf of the NHSBSP to provide an evaluation of the Fuji Amulet f/s Digital Breast Imaging System
Population affected	Women eligible for routine and higher-risk breast screening
Target audience	Physicists
Archived	Current document

CONTENTS

Authors.....	i
CONTENTS	iii
ACKNOWLEDGEMENTS.....	iv
EXECUTIVE SUMMARY.....	v
1 INTRODUCTION	1
1.1 Testing procedures and performance standards for digital mammography	1
1.2 Objectives.....	1
1.3 Limitations of this evaluation.....	1
2 METHODS.....	2
2.1 System tested.....	2
2.2 Output and half-value-layer (HVL)	3
2.3 Detector response	3
2.4 Dose measurement	3
2.5 Contrast to noise ratio (CNR).....	3
2.6 AEC performance for local dense areas	4
2.7 Noise analysis	5
2.8 Image quality measurements.....	6
2.9 Image retention.....	7
2.10 Physical measurements of the detector performance	7
2.11 Optimisation.....	7
3 RESULTS.....	9
3.1 Output and HVL.....	9
3.2 Detector response	9
3.3 AEC performance	9
3.4 Noise measurements.....	14
3.5 Image quality measurements.....	15
3.6 Comparison with other systems	18
3.7 Image retention.....	22
3.8 Detector performance	22
3.9 Optimisation.....	22
4 DISCUSSION	24
5 CONCLUSIONS	25
6 COMMENTS FROM MANUFACTURER.....	26
6.1 AEC performance	26
6.2 Filtering applied to images	26
REFERENCES.....	27

ACKNOWLEDGEMENTS

The authors are grateful to the staff at the Fujifilm Head Office in Bedford, UK for their help in evaluating the equipment at their site.

EXECUTIVE SUMMARY

The purpose of the evaluation was to determine whether the Fuji Amulet f and s breast imaging system meets the main standards set out in the NHSBSP and European protocols, and to provide performance data for comparison against other products.

This system is equipped with three dose modes (high, normal, and low). Doses in all three modes were below the remedial levels. There was a clear trade-off between the dose used and the image quality measured. In order to maintain image quality in excess of the achievable level, the high dose mode is recommended, especially for breast thicknesses in excess of about 50 mm. For lower breast thicknesses, normal dose mode would be sufficient. Used in this way (i.e. with sufficient dose) this system is capable of providing good image quality within current dose limits. Use of the low dose mode is not recommended.

1 INTRODUCTION

1.1 Testing procedures and performance standards for digital mammography

This report is one of a series evaluating commercially available digital mammography systems on behalf of the NHS Breast Screening Programme (NHSBSP). The testing methods and standards applied are mainly derived from NHSBSP Equipment Report 0604,¹ and are referred to in this document as 'the NHSBSP protocol'. The standards for image quality and dose are the same as those provided in the European protocol,^{2,3} but the latter has been followed where it provides a more detailed performance standard: for example, for the automatic exposure control (AEC) system.

1.2 Objectives

The purpose of these tests was to determine whether the Fuji Amulet f and s breast imaging system meets the main standards in the NHSBSP and European protocols, and to provide performance data for comparison against other products.

Practical evaluations are published separately by the NHSBSP for systems that meet the minimum standards in the NHSBSP protocol. A final decision on the suitability of systems for use in the NHSBSP depends on a review of both the technical and practical evaluations.

1.3 Limitations of this evaluation

After the tests were carried out, images understood to be unprocessed ('raw') were provided by Fujifilm for NCCPM to perform the analysis offsite, which is the normal procedure. However, detailed analysis showed that the images were not raw, but that some degree of processing had been applied to them. This was not fully understood until the information reproduced in section 6.2 was provided. Fujifilm now offer the option of truly unprocessed images, and some additional testing will be undertaken in due course so that an updated report can be published.

2 METHODS

2.1 System tested

The tests were conducted at the Fuji headquarters in Bedford, UK, on the system shown in Figure 1 and described in Table 1.



Figure 1 Photograph of Fuji Amulet f/s

Table 1 System Description

Manufacturer	Fuji
Model	Amulet f/s
System serial number	20008
Target material	Tungsten
Added filtration	50 ± 5 µm rhodium
Detector type	Amorphous selenium
Pixel size	50 µm (in detector plane)
Pixel array	Small: 3540 x 4740 Large: 4728 x 5928
Source to detector distance	650 mm
Source to table distance	633 mm
AEC modes	L-mode, N-mode and H-mode
AEC pre-exposure pulse	5-15 mAs depending on thickness and kV*
Software version	FDR-2000AWS Mainsoft V4.0

*The pre-pulse is included in the total mAs displayed on-screen and in the DICOM header; it contributes to the image.

2.2 Output and half-value-layer (HVL)

The output and HVL were measured as described in the NHSBSP protocol, at intervals of 3 kV for each target/filter combination.

2.3 Detector response

The detector response was measured as described in the NHSBSP protocol, with a 45 mm thickness of perspex (polymethylmethacrylate, or PMMA) placed at the tube exit port. An ion chamber was positioned above the table to determine the incident air kerma at the detector surface for a range of manually set mAs values at 28 kV with the W/Rh target/filter combination. The readings were corrected to the surface of the detector using the inverse square law. No correction was made for attenuation by the table and detector cover. Images were saved as unprocessed files and transferred to another computer for analysis. A 10 mm square region of interest (ROI) was positioned on the midline, 6 cm from the chest wall edge of each image. The average pixel value and the standard deviation of pixel values within that region were measured. The relationship between average pixel values and the detector entrance surface air kerma was determined.

2.4 Dose measurement

Doses were measured using the X-ray set's automatic exposure control (AEC) to expose different thicknesses of PMMA. Each thickness had an area of 18 x 24 cm. The paddle height was adjusted to be equal to the equivalent breast thickness. Mean glandular doses (MGDs) were calculated for the equivalent breast thicknesses.

2.5 Contrast to noise ratio (CNR)

A further set of images were acquired by the method described in section 2.4, but with the addition of a piece of aluminium foil to provide contrast. An aluminium square, 10 mm x 10 mm and 0.2 mm thick, was placed on top of a 20 mm thick block, with one edge on the midline, 6 cm from the chest wall edge. Additional layers of PMMA were placed on top of these to vary the total thickness.

The images were analysed to obtain the CNRs. Twenty small square ROIs (approximately 2.5 mm x 2.5 mm) were used to determine the average signal and the standard deviation in the signal within the image of the aluminium square (4 ROI) and the surrounding background (16 ROI), as shown in Figure 2. Small ROIs are used to minimise distortions due to the heel effect and other causes of non-uniformity.⁴ This is less important for DR systems than for computed radiography systems, however, because a flat-field correction is applied. The CNR was calculated for each image, as defined in the NHSBSP and European protocols.

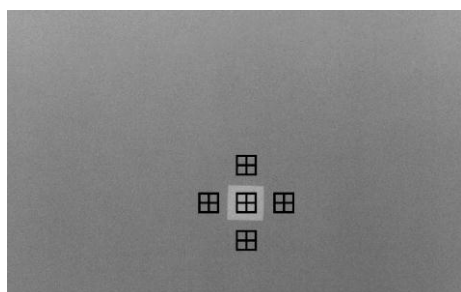


Figure 2 Location and size of ROI used to determine the CNR

To apply the standards in the European protocol, the limiting value for CNR (using 50 mm PMMA) was determined according to Equation 1. This equation determines the CNR value

($CNR_{limiting\ value}$) that is necessary to achieve the minimum threshold gold thickness for the 0.1 mm detail (i.e. $threshold\ gold_{limiting\ value} = 1.68\ \mu m$ which is equivalent to $threshold\ contrast_{limiting\ value} = 23.0\%$ using 28 kV Mo/Mo). Threshold contrasts were calculated as described in the European protocol and used in Equation 1.

$$CNR_{limiting\ value} = CNR_{measured} \times \frac{TC_{measured}}{TC_{limiting_value}} \tag{1}$$

The relative CNR was then calculated according to Equation 2 and compared with the limiting values provided for relative CNR shown in Table 2. The minimum CNR required to meet this criterion was then calculated.

$$Relative\ CNR = CNR_{measured} / CNR_{limiting\ value} \tag{2}$$

Table 2 Limiting values for relative CNR

Thickness of PMMA (mm)	Equivalent breast thickness (mm)	Limiting values for relative CNR (%) in European protocol
20	21	>115
30	32	>110
40	45	>105
45	53	>103
50	60	>100
60	75	> 95
70	90	> 90

2.6 AEC performance for local dense areas

The method used in the EUREF type testing protocol was followed. To simulate local dense areas, nine images were made with different thicknesses (2-18 mm) of PMMA providing extra attenuation, so that the compression plate remained in position at 40 mm height, as shown in Figure 3.

In the area of the extra attenuation (20 x 40 mm PMMA), the mean pixel value and standard deviation of a ROI 2.5 x 2.5 mm ROI were measured, and the signal-to-noise ratio (SNR) calculated. The background pixel value outside the extra attenuation region was also determined.

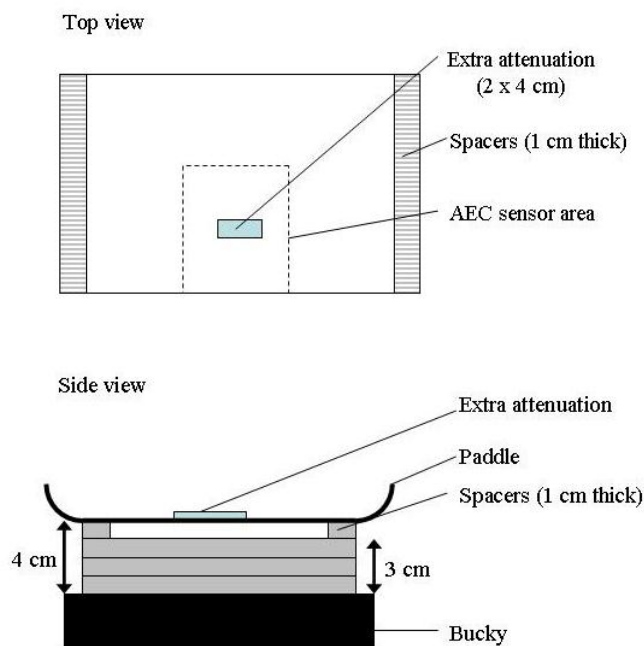


Figure 3 Setup to measure AEC performance for local dense areas

2.7 Noise analysis

The images acquired in the measurements of detector response using 28 kV W/Rh were used to analyse the image noise. Small ROI with an area of approximately 2.5 x 2.5 mm were placed on the midline and 6 cm from the chest wall edge in each image. The average standard deviations of the pixel values in these ROI for each image were used to investigate the relationship between the dose to the detector and the image noise. It was assumed that this noise comprises three components; electronic noise, structural noise, and quantum noise, with the relationship shown in Equation 3:

$$\sigma_p = \sqrt{k_e^2 + k_q^2 p + k_s^2 p^2} \tag{3}$$

where σ_p is the standard deviation in pixel values within an ROI with a uniform exposure and a mean pixel value p , and k_e , k_q , and k_s are the coefficients determining the amount of electronic, quantum, and structural noise in a pixel with a value p . This method of analysis has been described previously.⁵ For simplicity, the noise is generally presented here as relative noise, defined as in Equation 4.

$$\text{Relative noise} = \frac{\sigma_p}{p} \tag{4}$$

The variation in relative noise with mean pixel value was evaluated and fitted using Equation 3, and non-linear regression used to determine the best fit for the constants and their asymptotic confidence limits (using Graphpad Prism Version 5.02 for Windows)*. This established whether the experimental measurements of the noise fitted this equation, and

* Graphpad software, San Diego, California, USA, www.graphpad.com

the relative proportions of the different noise components. In fact, the relationship between noise and pixel values has been found empirically to be approximated by a simple power relationship as shown in Equation 5:

$$\frac{\sigma_p}{p} = k_t p^{-n} \quad (5)$$

where k_t is a constant. If the noise were purely quantum noise, the value of n would be 0.5. However the presence of electronic and structural noise means that n can be slightly higher or lower than 0.5.

2.8 Image quality measurements

Contrast detail measurements were made using the CDMAM phantom (version 3.4, serial number 1022).[†] The phantom was positioned with a 20 mm thickness of PMMA above and below, to give a total attenuation approximately equivalent to 50 mm of PMMA or 60 mm thickness of typical breast tissue. The kV target/filter combination and mAs were chosen to match as closely as possible those selected by the AEC when imaging a 5 cm thickness of PMMA. This procedure was repeated to obtain a representative sample of 16 images at this dose level. Further images of the test phantom were then obtained at other dose levels by manually selecting higher and lower mAs values with the same beam quality. Images were transferred to disk for subsequent analysis off-site.

An automatic method of reading the CDMAM images was used.^{5,6} The threshold gold thickness for a typical human observer was predicted using Equation 6:

$$TC_{predicted} = r TC_{auto} \quad (6)$$

where $TC_{predicted}$ is the predicted threshold contrast for a typical observer and TC_{auto} is the threshold contrast measured using an automated procedure with CDMAM images. Contrasts were calculated from gold thickness for a nominal tube voltage of 28 kV and a Mo/Mo target filter combination as described in the European protocol; r is the average ratio between human and automatic threshold contrast determined experimentally with the values shown in Table 3.⁶

Table 3 Values of r used to predict threshold contrast

Diameter of gold disc (mm)	Average ratio of human to automatically measured threshold contrast (r)
0.08	1.40
0.10	1.50
0.13	1.60
0.16	1.68
0.20	1.75
0.25	1.82
0.31	1.88
0.40	1.94
0.50	1.98
0.63	2.01
0.80	2.06
1.00	2.11

[†] UMC St. Radboud, Nijmegen University, Netherlands

The main advantage of automatic reading is that it has the potential to eliminate observer error, which is a significant problem when using human observers. However it should be noted that at the present time the official protocols are based on human reading.

The predicted threshold gold thickness for each detail diameter at each dose level was fitted with a curve, as described in the NHSBSP protocol. The confidence limits for the predicted threshold gold thicknesses have been previously determined by a resampling method using a large set of images. The threshold contrasts quoted in the tables of results are derived from the fitted curves, as this has been found to improve accuracy.⁶

The expected relationship between threshold contrast and dose is shown in Equation 7.

$$\text{Threshold contrast} = \lambda D^{-n} \quad (7)$$

where D represents the MGD for a 60 mm thick standard breast equivalent to the test phantom configuration used for the image quality measurement, and λ is a constant to be fitted. It is assumed that a similar equation applies when using threshold gold thickness instead of contrast. This equation was plotted with the experimental data for each detail size from 0.1 mm to 1.0 mm. The value of n resulting in the best fit to the experimental data was determined.

2.9 Image retention

Image retention was measured as described in the NHSBSP protocol. The regions used are shown in Figure 4. The image retention factor was calculated using Equation 8.

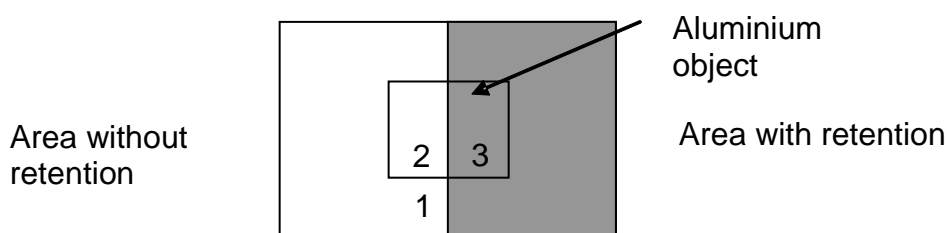


Figure 4 ROIs used for calculation of the image retention factor

$$\text{Image retention factor} = \frac{\text{mean pixel value (region 3)} - \text{mean pixel value (region 2)}}{\text{mean pixel value (region 1)} - \text{mean pixel value (region 2)}} \quad (8)$$

2.10 Physical measurements of the detector performance

The modulation transfer function (MTF), normalised noise power spectrum (NNPS) and the detective quantum efficiency (DQE) of the detector were measured, but the results are not presented in this version of the report because the images were not unprocessed (see section 1.3 for details).

2.11 Optimisation

A method for determining optimal beam qualities and exposure factors for digital mammography systems has been described previously and was used to evaluate this system.^{4,5} CNR and MGD were measured as described above, using 20 to 70 mm thick blocks of PMMA. For each thickness, a range of voltage settings were used and the post-exposure mAs values were recorded. The MGDs to typical breasts with attenuation equivalent to each thickness of the PMMA were calculated, as described in the NHSBSP

protocol. Each exposure was designed to achieve a standard pixel value. The relationship between noise and pixel values in digital mammography systems has been previously shown to be approximated by⁵:

$$\text{Relative noise} = \frac{\sqrt{\frac{sd(bgd)^2 + sd(AI)^2}{2}}}{p} = k_t p^{-n} \quad (8)$$

where k_t is a constant, p is the average background pixel value linearised with absorbed dose to the detector, $sd(bgd)$ is the average standard deviation of pixel values in the ROIs over the background, and $sd(AI)$ is the average standard deviation of pixel values in an ROI over a 0.2 mm x 10 mm x 10 mm piece of aluminium. The value of n was found by fitting this equation to the experimental data. Equation 9 was then used to calculate the dose required to achieve a target CNR, where k is a constant to be fitted, and D is the MGD for a breast of equivalent thickness:

$$\text{CNR} = k D^n \quad (9)$$

The target CNR was that calculated to reach either the minimum or achievable image quality as specified in the NHSBSP and European protocols using the following relationship:

$$\text{Threshold contrast} = \frac{\lambda}{\text{CNR}} \quad (10)$$

where λ is a constant that is independent of dose, beam quality and the thickness of attenuating material. The optimal beam quality for each thickness was selected as that necessary to achieve the target CNR for the minimum dose.

3 RESULTS

3.1 Output and HVL

The results are shown in Table 4.

Table 4 Output and HVL

kV Target/Filter	Output ($\mu\text{Gy}/\text{mAs}$ at 1 m)	HVL (mm Al)
25 W/Rh	12.3	0.48
28 W/Rh	16.8	0.51
31 W/Rh	21.2	0.53
34 W/Rh	25.7	0.55

3.2 Detector response

The detector was found to have a logarithmic response, as shown in Figure 5.

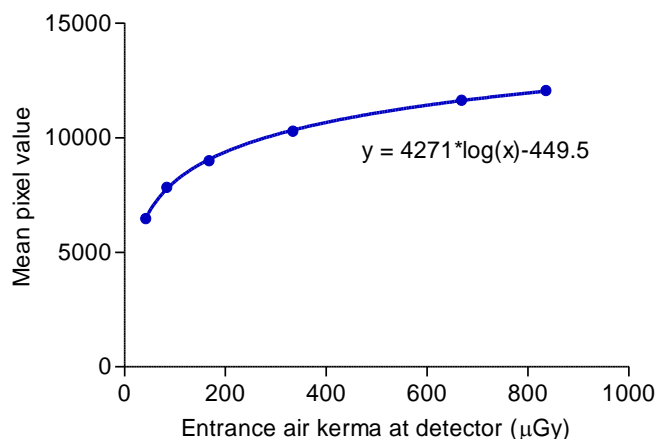


Figure 5 Detector response

3.3 AEC performance

3.3.1 Dose

There are three different AEC modes: H (high), N (normal), and L (low). The MGDs for breasts simulated with PMMA exposed under AEC control are shown in Table 5 and Figure 6. At all thicknesses, the dose was below the remedial level in the NHSBSP protocol, which is the same as the maximum acceptable level in the European protocol. For the H mode, the MGD was very close to the remedial level for the smallest thicknesses (21 and 32 mm equivalent breast).

The pre-exposure pulse used in AEC modes ranged between 5 and 15 mAs, depending on kV and compressed breast thickness. Besides contributing to the MGD, this is used with the main exposure to produce the digital image, and is included in the displayed mAs and the value stored in the DICOM header.

The MGD values stored in the DICOM header (last column of table 5, original values in dGy) are clearly different from those which were calculated in this evaluation, according to the UK and European protocols.

Table 5a Mean glandular dose for simulated breasts (N mode)

PMMA thickness (mm)	Equivalent breast thickness (mm)	kV	target	filter	mAs	MGD (mGy)	NHSBSP remedial level (mGy)	MGD value in DICOM header (mGy)
20	21	26	W	Rh	36.4	0.62	> 1.0	0.49
30	32	27	W	Rh	59.9	0.91	> 1.5	0.68
40	45	28	W	Rh	77.9	1.10	> 2.0	0.74
45	53	29	W	Rh	88.3	1.27	> 2.5	0.83
50	60	30	W	Rh	96.0	1.42	> 3.0	0.88
60	75	31	W	Rh	141.2	1.98	> 4.5	1.17
70	90	32	W	Rh	203.1	2.71	> 6.5	1.56

Table 5b Mean glandular dose for simulated breasts (H mode)

PMMA thickness (mm)	Equivalent breast thickness (mm)	kV	target	filter	mAs	MGD (mGy)	NHSBSP remedial level (mGy)	MGD value in DICOM header (mGy)
20	21	26	W	Rh	54.0	0.92	> 1.0	0.73
30	32	27	W	Rh	89.0	1.36	> 1.5	1.00
40	45	28	W	Rh	114.0	1.61	> 2.0	1.08
45	53	29	W	Rh	129.5	1.86	> 2.5	1.21
50	60	30	W	Rh	141.3	2.09	> 3.0	1.30
60	75	31	W	Rh	210.2	2.95	> 4.5	1.74
70	90	32	W	Rh	303.4	4.05	> 6.5	2.33

Table 5c Mean glandular dose for simulated breasts (L mode)

PMMA thickness (mm)	Equivalent breast thickness (mm)	kV	target	filter	mAs	MGD (mGy)	NHSBSP remedial level (mGy)	MGD value in DICOM header (mGy)
20	21	27	W	Rh	24.1	0.46	> 1.0	0.32
30	32	27	W	Rh	37.9	0.58	> 1.5	0.43
40	45	28	W	Rh	49.1	0.69	> 2.0	0.47
45	53	29	W	Rh	58.1	0.83	> 2.5	0.54
50	60	30	W	Rh	61.4	0.91	> 3.0	0.56
60	75	31	W	Rh	90.1	1.26	> 4.5	0.74
70	90	32	W	Rh	134.6	1.80	> 6.5	1.03

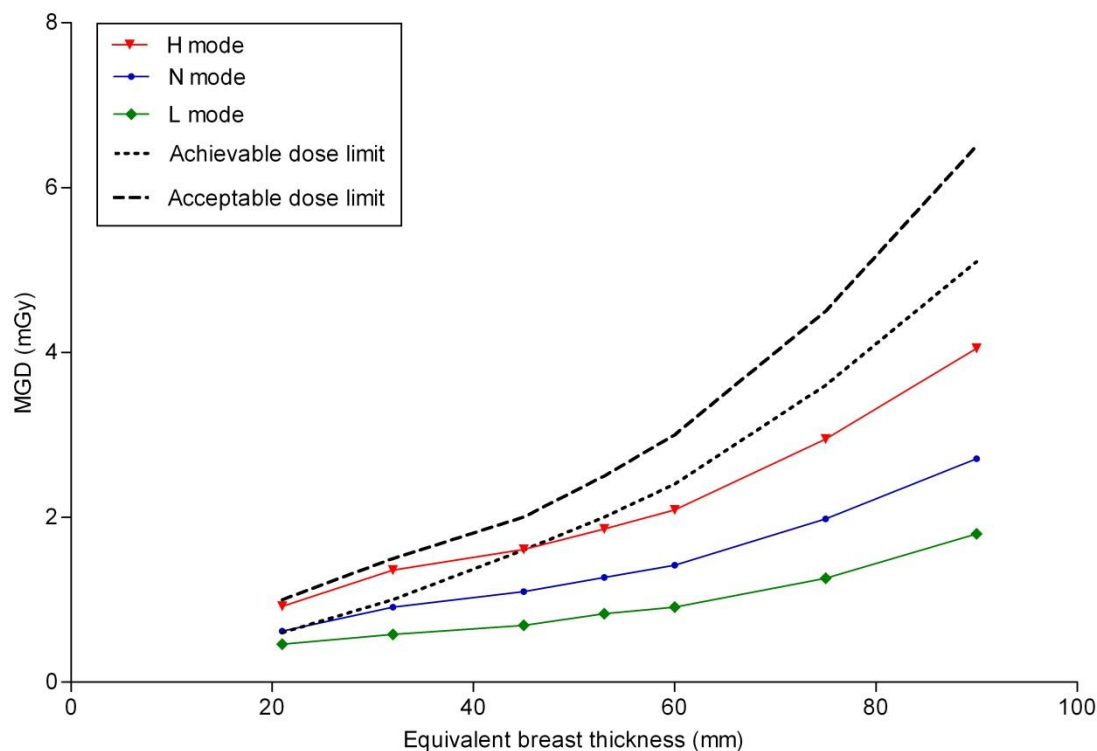


Figure 6 MGD for different thicknesses of simulated breasts for the three different AEC modes

3.3.2 CNR

The results of the contrast and CNR measurements are shown in Table 6 and Figure 7. The CNRs required to meet the minimum acceptable and achievable image quality standards at the 60 mm breast thickness have been calculated and are also shown in Table 6 and Figure 7. The CNR required at each thickness to meet the limiting values for CNR in the European protocol are also shown.

Table 6a Contrast and CNR measurements using AEC (N mode)

Equivalent breast thickness (mm)	kV Target/Filter	mAs	Back-ground pixel value*	% contrast for 0.2 mm Al	Measured CNR	CNR at minimum acceptable IQ	CNR at achievable IQ	CNR to meet Euro limiting value	European limiting values for relative CNR
21	26 W Rh	37.9	150	16.2%	16.4	6.27	9.24	7.21	> 115
32	27 W Rh	58.7	144	15.2%	15.1	6.27	9.24	6.90	> 110
45	28 W Rh	78.0	121	14.2%	12.6	6.27	9.24	6.58	> 105
53	29 W Rh	90.1	121	13.6%	12.0	6.27	9.24	6.46	> 103
60	30 W Rh	96.1	113	12.9%	10.8	6.27	9.24	6.27	> 100
75	31 W Rh	141.1	116	11.9%	9.8	6.27	9.24	5.96	> 95
90	32 W Rh	207.4	121	10.6%	8.8	6.27	9.24	5.64	> 90

Table 6b Contrast and CNR measurements using AEC (H mode)

Equivalent breast thickness (mm)	kV Target/Filter	mAs	Back-ground pixel value*	% contrast for 0.2 mm Al	Measured CNR	CNR at minimum acceptable IQ	CNR at achievable IQ	CNR to meet Euro. limiting value	European limiting values for relative CNR
21	26 W Rh	55.1	214	15.8%	20.7	6.54	9.64	7.21	> 115
32	27 W Rh	89.1	216	14.8%	19.3	6.54	9.64	6.90	> 110
45	28 W Rh	119.0	187	13.9%	16.3	6.54	9.64	6.58	> 105
53	29 W Rh	129.6	175	13.3%	14.7	6.54	9.64	6.46	> 103
60	30 W Rh	144.1	172	12.8%	13.8	6.54	9.64	6.27	> 100
75	31 W Rh	206.4	167	11.6%	12.0	6.54	9.64	5.96	> 95
90	32 W Rh	311.4	180	10.6%	12.7	6.54	9.64	5.64	> 90

Table 6c Contrast and CNR measurements using AEC (L mode)

Equivalent breast thickness (mm)	kV Target/Filter	mAs	Back-ground pixel value*	% contrast for 0.2 mm Al	Measured CNR	CNR at minimum acceptable IQ	CNR at achievable IQ	CNR to meet Euro. limiting value	European limiting values for relative CNR
21	27 W Rh	23.7	92	16.4%	12.5	6.05	8.93	7.2	> 115
32	27 W Rh	38.7	94	15.2%	11.6	6.05	8.93	6.9	> 110
45	28 W Rh	49.1	76	14.2%	9.4	6.05	8.93	6.6	> 105
53	29 W Rh	58.1	78	13.8%	9.2	6.05	8.93	6.5	> 103
60	30 W Rh	62.5	74	13.2%	8.4	6.05	8.93	6.3	> 100
75	31 W Rh	94.1	75	11.8%	7.5	6.05	8.93	6.0	> 95
90	32 W Rh	134.6	79	10.8%	6.9	6.05	8.93	5.6	> 90

* Pixel values have been linearised.

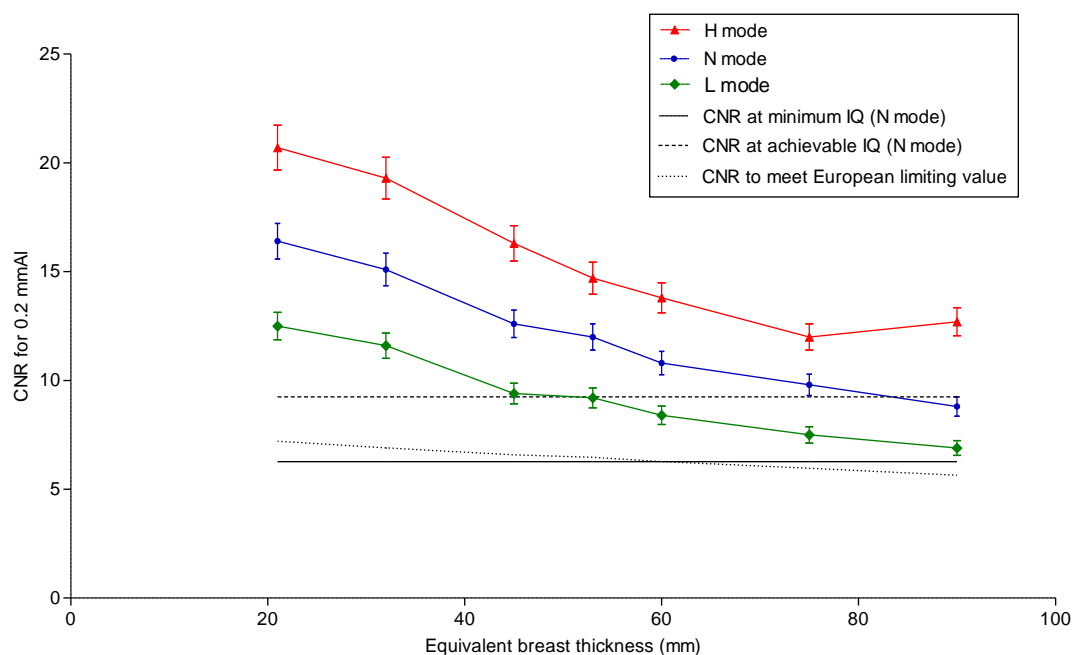


Figure 7 Measured CNR compared with the limiting values in the European protocol for the system (Error bars indicate 95% confidence limits)

3.3.3 AEC performance for local dense areas

The results presented in Table 7 and Figure 8 show the change in SNR and background pixel value, with increasing thickness of PMMA.

The Amulet f/s is designed to prevent a single high dense area from negatively influencing the dose given to the whole breast, rather than to maintain a constant SNR (which is what the EUREF test is designed to evaluate). Further explanation is provided in section 6.1.

Results are presented here for information but no criticism of the system is implied.

Table 7 AEC performance for local dense areas – N mode

Attenuation (mm PMMA)	Target/ Filter	Tube voltage (kV)	Tube load (mAs)	SNR	Background pixel value (linearised)
32	W/Rh	28	41.9	78.5	121.7
34	W/Rh	28	42.7	76.5	120.8
36	W/Rh	28	43.5	69.8	121.8
38	W/Rh	28	45.1	65.0	125.2
40	W/Rh	28	52.1	68.0	143.8
42	W/Rh	28	54.0	60.1	149.6
44	W/Rh	28	53.1	63.8	146.7
46	W/Rh	28	58.6	58.7	161.3
48	W/Rh	28	61.1	56.3	167.5

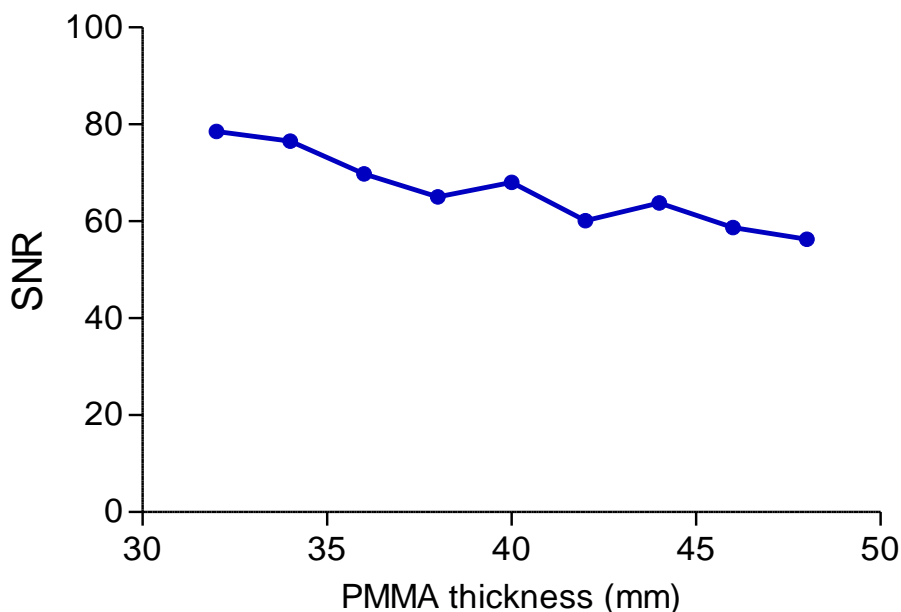


Figure 8a AEC performance for local dense areas (SNR)

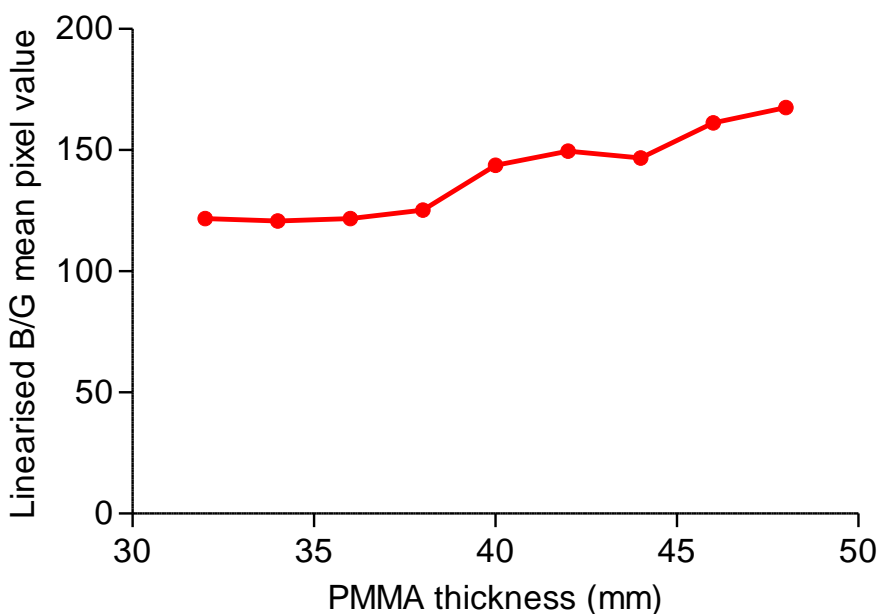


Figure 8b AEC performance for local dense areas (background pixel value, linearised)

3.4 Noise measurements

The variation in noise with dose was analysed by plotting the standard deviation in pixel values against the detector entrance air kerma, as shown in Figure 9. If quantum noise sources alone were present, the data would form a straight line with an index of 0.5. The index of the fit to this data (0.34) indicates the presence of some additional noise.

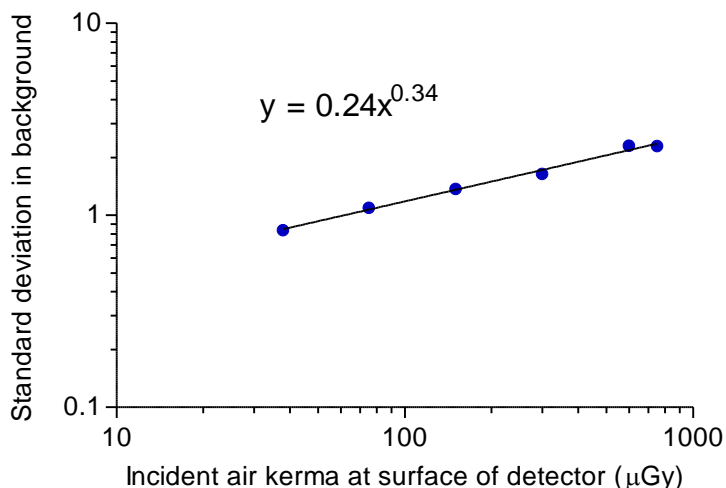


Figure 9 Standard deviation of pixel values versus air kerma at detector

Figure 10 is an alternative way of presenting the data and shows the relative noise at different entrance air kerma. The estimated relative contributions of electronic, structural, and quantum noise are shown and the quadratic sum of these contributions fitted to the measured noise (using Equation 3). The structural noise was found to be negligible.

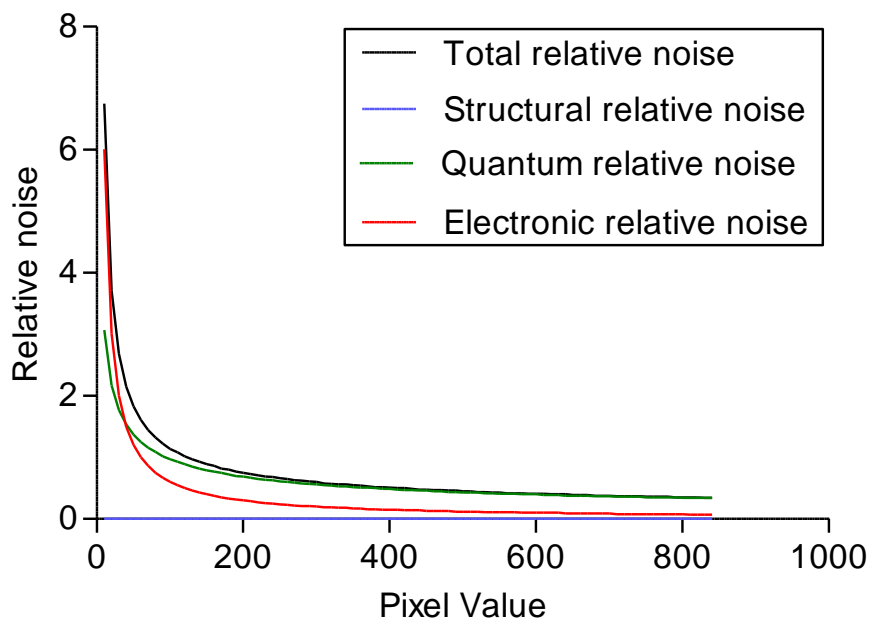


Figure 10 Relative noise and noise components at different pixel values.

3.5 Image quality measurements

The first exposures of the image quality phantom were made using the AEC in N (normal) mode to select the beam quality and exposure factors. This resulted in the selection of 30 kV W/Rh and 90.1 mAs, giving a MGD of 1.33 mGy to an equivalent breast (60 mm thick). Subsequent image quality measurements were made by manual selection, at a range of mAs values between approximately half and double the AEC-selected mAs at the same beam quality, as shown in Table 8.

Table 8 Images acquired for image quality measurement

Exposure mode	kV target/filter	Tube loading (mAs)	MGD to equivalent breasts 60 mm thick (mGy)	Number of CDMAM images acquired and analysed
manual	30 W/Rh	45	0.67	16
manual	30 W/Rh	71	1.05	16
manual	30 W/Rh	90.1	1.33	16
manual	30 W/Rh	140.1	2.08	16
manual	30 W/Rh	180.3	2.67	16

The contrast detail curves at the different dose levels (determined by automatic reading of the images) are shown in Figure 11. The threshold gold thicknesses for different diameters and the different dose levels are shown in Table 9, along with the minimum and achievable threshold values from the NHSBSP protocol (which are the same as the European protocol). The data in Table 9 are taken from the raw data rather than the fitted curve.

The measured threshold gold thicknesses are plotted against the MGD for an equivalent breast for the 0.1 and 0.25 mm detail sizes in Figure 12. The curves in Figure 12 were interpolated to find the doses required to meet the minimum acceptable and achievable threshold gold thicknesses shown in Tables 10 and 11. A similar procedure was used to determine the doses required to meet the minimum acceptable and achievable image quality levels for detail sizes from 0.1 to 1.0 mm, as shown in Figure 13.

Table 9 Average threshold gold thicknesses for different detail diameters for five doses using 30 kV W/Rh and automatically predicted data.

Diameter (mm)	Threshold gold thickness (μm)						
	Acceptable value	Achievable value	MGD= 0.67 mGy	MGD= 1.05 mGy	MGD= 1.33 mGy	MGD= 2.08 mGy	MGD= 2.67 mGy
0.1	1.680	1.100	2.031 ± 0.135	1.343 ± 0.097	0.966 ± 0.069	0.801 ± 0.062	0.660 ± 0.047
0.25	0.352	0.244	0.332 ± 0.024	0.291 ± 0.021	0.253 ± 0.017	0.223 ± 0.015	0.200 ± 0.013
0.5	0.150	0.103	0.163 ± 0.012	0.130 ± 0.011	0.115 ± 0.009	0.083 ± 0.007	0.086 ± 0.007
1	0.091	0.056	0.085 ± 0.009	0.074 ± 0.008	0.071 ± 0.008	0.054 ± 0.006	0.050 ± 0.005

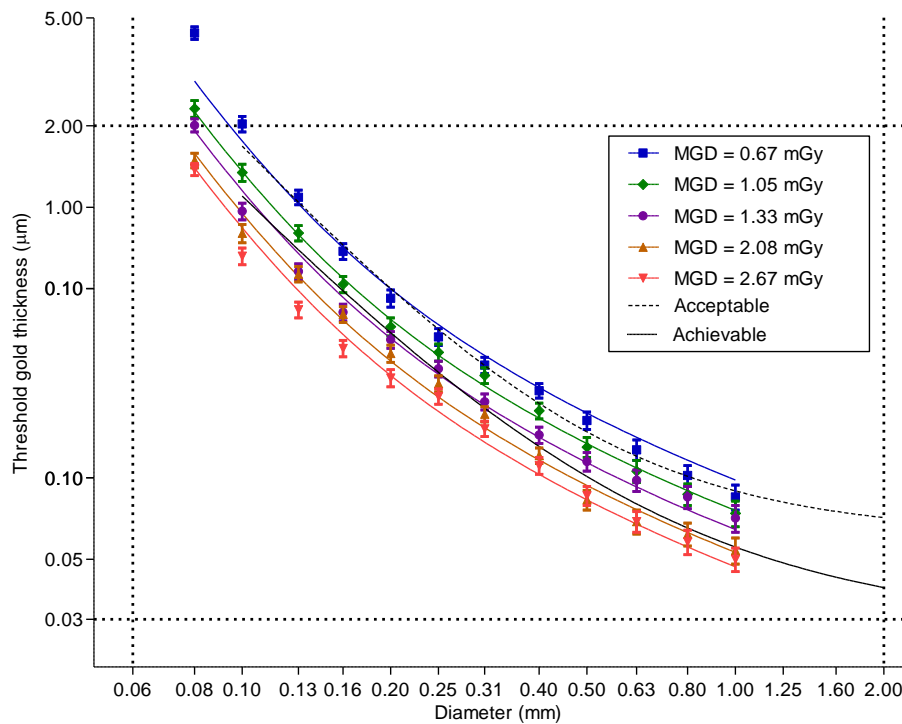


Figure 11 Contrast-detail curves for five doses at 30 kV W/Rh using predicted results from automated reading. The 1.33 mGy dose corresponds to the AEC selection. Error bars indicate 95% confidence limits.

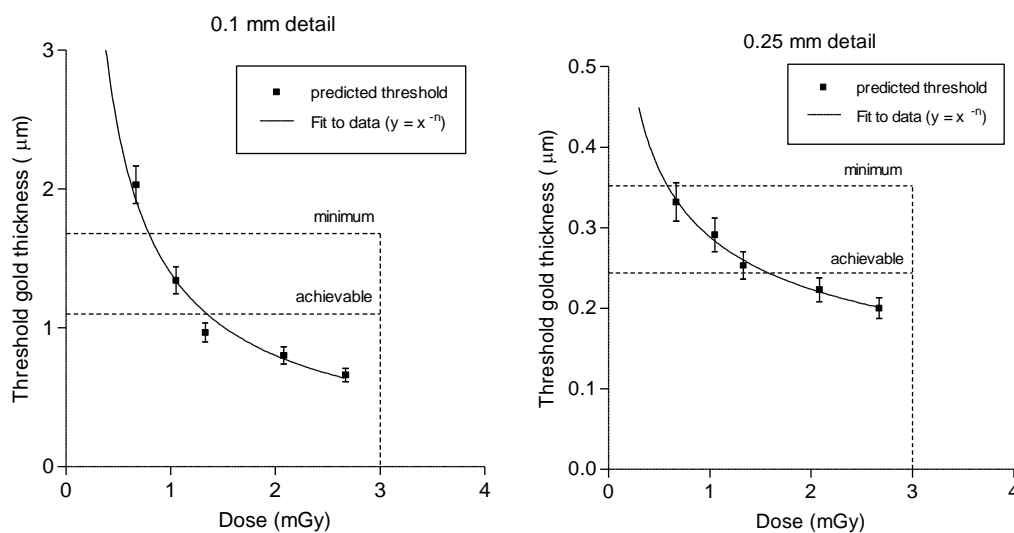


Figure 12 Threshold gold thickness at different doses. Error bars indicate 95% confidence limits. The doses are for a breast equivalent to a 5 cm thickness of PMMA.

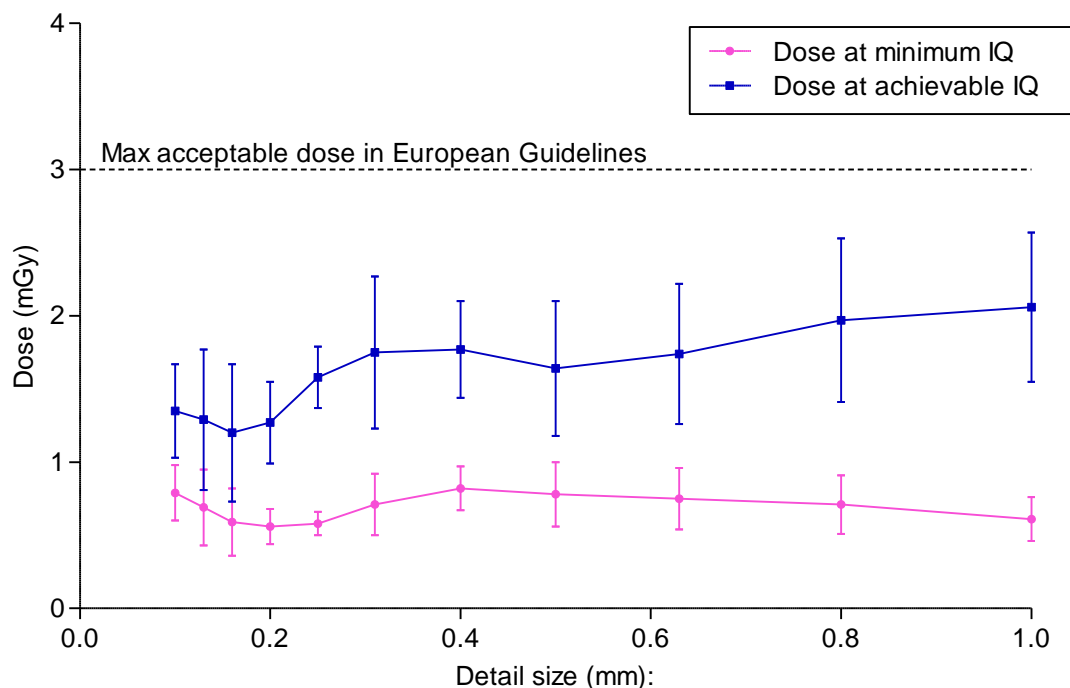


Figure 13 The MGD calculated to be necessary to reach the achievable and minimum acceptable image quality levels at different detail sizes using 30 kV W/Rh for an equivalent breast 60 mm thick. Based on predicted threshold gold thicknesses.

3.6 Comparison with other systems

The MGDs to reach the minimum and achievable image quality standards in the NHSBSP protocol have been estimated from the curves shown in Figure 12. (The error in estimating these doses depends on the accuracy of the curve fitting procedure, and pooled data for several systems has been used to estimate the 95% confidence limits of about 20%). These doses are shown against similar data for other models of digital mammography system in Tables 10 and 11 and Figures 14 to 17. The data for the other systems has been determined in the same way as described in this report. The results were published previously.⁷⁻¹⁷ The data for film screens represents an average value, which was determined using a variety of modern film screen systems.

Table 10 The MGD required to reach the minimum threshold gold thickness for 0.1 mm and 0.25 mm details for different systems.

System	MGD (mGy) for 0.1 mm		MGD (mGy) for 0.25 mm	
	Human	Predicted	Human	Predicted
Philips (Sectra) MicroDose L30		0.61		0.49
Siemens Inspiration	0.97	0.76	0.87	0.60
Fuji Amulet 1	0.62	0.67	0.74	0.71
Fuji Amulet f/s		0.79		0.58
Hologic Dimensions	0.56	0.38	0.65	0.40
Hologic Selenia (W)	0.58	0.71	0.65	0.64
GE Essential	0.60	0.49	0.50	0.49
GE DS	1.01	0.82	0.87	0.83
IMS Giotto (W)	1.07	1.38	0.91	1.17
Film-screen	1.17	1.30	1.07	1.36
Agfa CR85-X (NIP)	1.24	1.27	1.06	0.96
Agfa CR (MM3.0) [†]	2.54	2.32	1.45	1.54
Fuji Profect CR	1.67	1.78	1.45	1.35
Carestream CR (EHR-M2)	2.29	2.34	1.45	1.80
Konica Minolta CR (CP-1M) NIP	1.60	1.47	1.12	0.99

[†]Data are the mean of measurements shown in NHSBSP Equipment Reports 0707⁸ and 0905.¹⁴

Table 11 The MGD required to reach the achievable threshold gold thickness for 0.1 and 0.25 mm details for different systems.

System	MGD (mGy) for 0.1 mm		MGD (mGy) for 0.25 mm	
	Human	Predicted	Human	Predicted
Philips (Sectra) MicroDose L30		1.47		1.05
Siemens Inspiration	2.06	1.27	1.68	1.16
Fuji Amulet 1	1.40	1.13	1.50	1.41
Fuji Amulet f/s		1.35		1.58
Hologic Dimensions	1.29	0.91	1.23	0.85
Hologic Selenia (W)	1.66	1.37	1.61	1.48
GE Essential	1.57	1.13	1.14	1.03
GE DS	2.35	1.57	1.80	1.87
IMS Giotto (W)	2.33	2.73	1.77	2.11
Film-screen	2.48	3.03	2.19	2.83
Agfa CR (NIP)	3.22	2.47	2.40	2.34
Agfa CR (MM3.0)	5.21	5.14	3.72	3.82
Fuji Profect CR	4.26	3.29	3.52	2.65
Carestream CR (EHR-M2)	5.34	5.45	3.03	3.74
Konica Minolta CR (CP-1M) NIP	4.53	3.45	2.73	2.08

[†]Data are the mean of measurements shown in NHSBSP Equipment Reports 0707⁸ and 0905.¹⁴

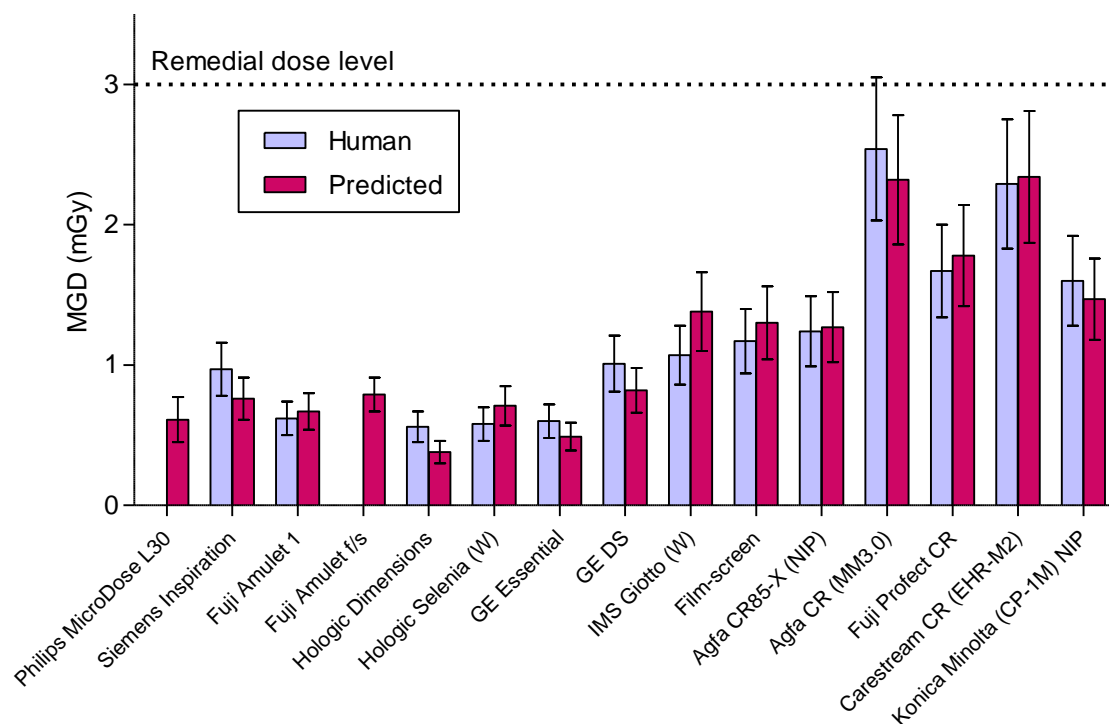


Figure 14 Dose to reach minimum acceptable image quality standard for 0.1 mm detail. Error bars indicate 95% confidence limits.

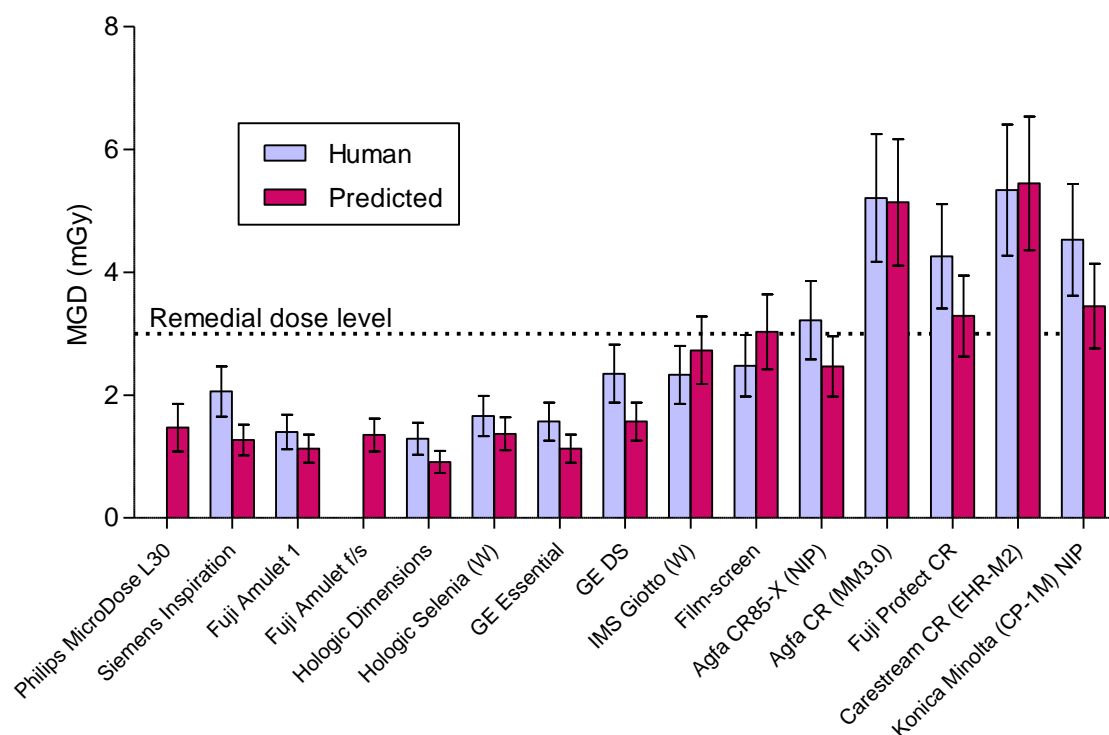


Figure 15 Dose to reach achievable image quality standard for 0.1 mm detail. Error bars indicate 95% confidence limits.

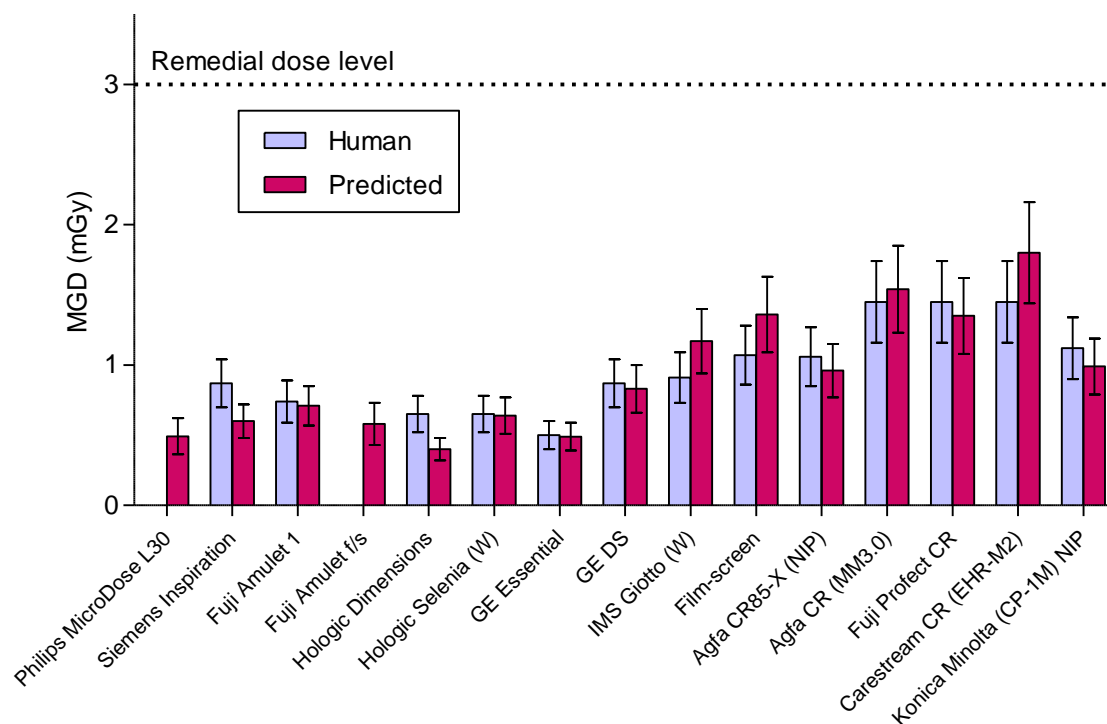


Figure 16 Dose to reach minimum acceptable image quality standard for 0.25 mm detail. Error bars indicate 95% confidence limits.

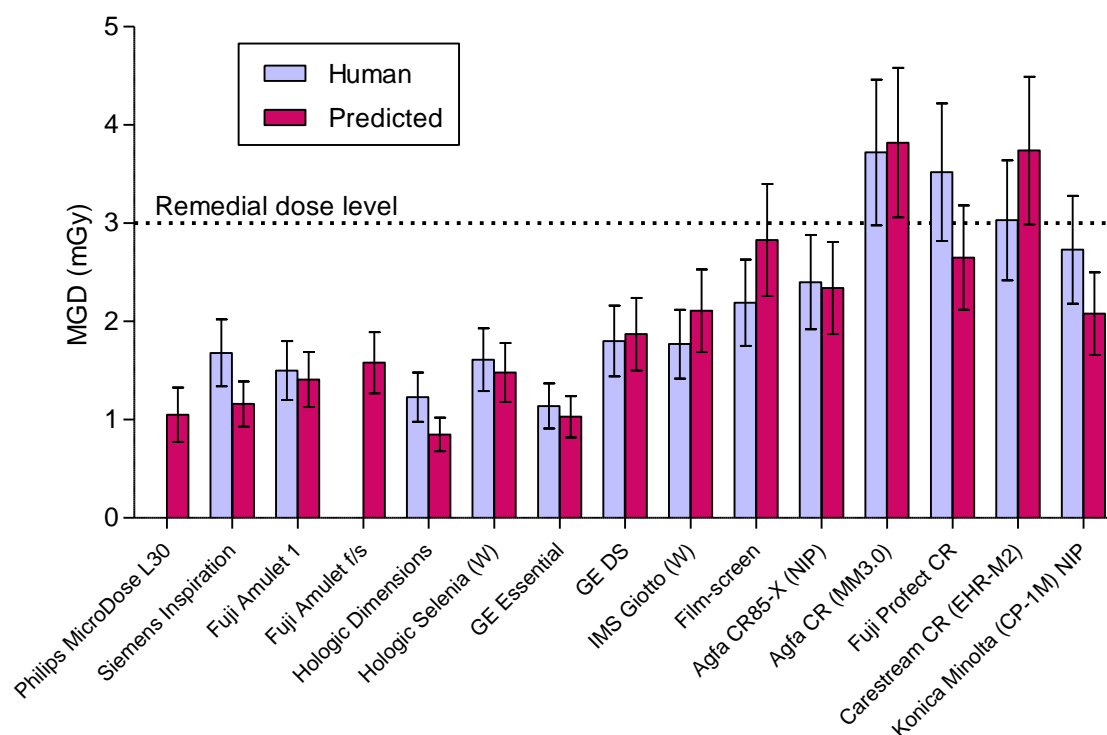


Figure 17 Dose to reach achievable image quality standard for 0.25 mm detail. Error bars indicate 95% confidence limits.

3.7 Image retention

The results are shown in Table 18. The image retention factor (0.021) is well below the remedial level (0.3).

Table 18 Image retention factor

ROI	pixel value
1	8368
2	8234
3	8231
image retention factor: 0.021	

3.8 Detector performance

The MTF and DQE results are not presented here but will be included in a future report.

3.9 Optimisation

The target CNR corresponding to the achievable image quality was calculated to be 9.2. The MGD required to reach this target CNR for each beam quality and different thicknesses of PMMA is shown in Figure 18. From this data, the optimal beam qualities were selected and are shown in Table 19. For smaller breast thicknesses, the factors suggested would result in dose savings of up to 58%.

Table 19 Optimal factors to produce achievable image quality (where CNR = 9.2)

PMMA Thickness	kV target/ filter	mAs	MGD (mGy)	MGD (mGy) when AEC selected factors used	% change in dose if optimal factors used (cf AEC selection)	Remedial dose level in NHSBSP protocol (mGy)
20	28 W Rh	31	0.26	0.62	-58%	1.0
30	25 W Rh	69	0.44	0.91	-52%	1.5
40	25 W Rh	115	0.68	1.10	-38%	2.0
45	28 W Rh	92	0.86	1.27	-32%	2.5
50	28 W Rh	101	1.11	1.42	-22%	3.0
60	29 W Rh	175	1.82	1.98	-8%	4.5
70	33 W Rh	206	2.59	2.71	-5%	6.5

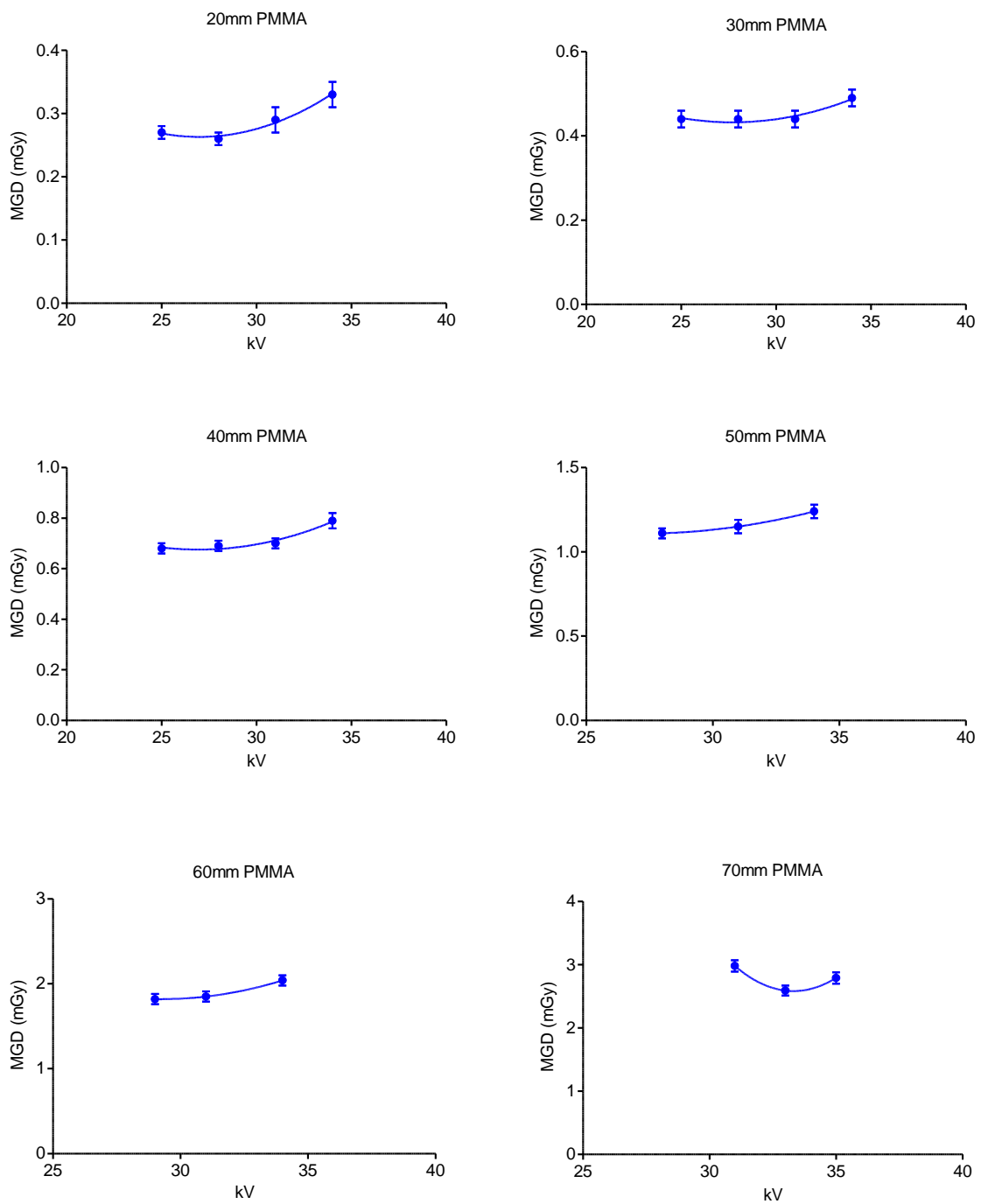


Figure 18 MGD to reach the achievable image quality standard in the NHSBSP protocol. Error bars indicate 95% confidence limits.

4 DISCUSSION

The detector response was logarithmic, in agreement with the manufacturer's specification.

The images provided for analysis had had some processing applied, as explained in sections 1.3 and 6.2. Further testing will be carried out in future to acquire unprocessed images, which will allow MTF and DQE to be determined. The image quality will also be re-evaluated.

Exposure under AEC resulted in doses to simulated breasts that were below the limits outlined in the NHSBSP protocol for all three AEC settings (N mode, H mode, and L mode). The doses to the standard breast simulated with 45 mm of PMMA were 1.27 mGy, 1.86 mGy and 0.83 mGy respectively for the N, H, and L modes. At this thickness, an upper limit of 2.5 mGy is applied by the NHSBSP. The MGDs calculated by the system were different from those calculated in this evaluation according to the Dance equation.

The three AEC modes resulted in background linearised pixel values that varied between 74 and 216, depending on the thickness and mode used. For all three modes the tube voltage ranged from 26 to 32 kV. The net result of these choices was that the CNR values were relatively high for thinner breasts but dropped with increasing breast thickness. All three AEC modes exceeded the minimum requirements of the European protocol. However, for N and L modes, the CNR values fell below that necessary to reach the achievable level of image quality for the larger thicknesses. When adding extra PMMA to simulate a denser area in the breast, a gradual decrease in SNR was observed.

The noise analysis showed that there was some electronic noise, while structural noise appeared negligible.

The image quality measurements indicated that, for the standard thickness tested (equivalent to 50 mm thickness of PMMA, i.e. 60 mm of typical breast) the image quality was close to the achievable level in normal mode, except for the larger details (0.4 mm and above) for which it fell below this level. In N mode, the AEC selected a dose of 1.33 mGy using 30 kV W/Rh. A dose of about 0.61 ± 0.12 mGy was calculated to be necessary to reach the minimum image quality level at the 0.1 mm detail size for this equivalent breast thickness. A dose of about 1.36 ± 0.27 mGy was calculated to be necessary to reach the achievable image quality level for this equivalent breast thickness at the 0.1 mm detail size.

The doses required to reach acceptable and achievable image quality levels are comparable to those measured for other digital mammography (DR) systems.

The image retention factor, 0.021, is well below the remedial level of 0.3.

The results of the optimisation study suggest that 25 kV W/Rh would be optimum for smaller breasts, 28 kV W/Rh for medium sized breasts, and 33 kV W/Rh for the largest breasts.

5 CONCLUSIONS

The Fuji Amulet f/s system is capable of producing good image quality at a relatively low radiation dose. The system met the dose standards in the NHSBSP and European protocols, and the image quality standards were also met, as determined using the images provided. Further testing will be carried out using the new software version to acquire unprocessed images and an updated report will be published.

6 COMMENTS FROM MANUFACTURER

Fujifilm has supplied explanatory information on some aspects of the Amulet's performance, which is reproduced here:

6.1 AEC performance

The SNR difference seen in the Amulet f/s is a result of the different design of the AEC control on the system compared to other manufacturers' units. Fujifilm's AEC control algorithm is designed to prevent a very small high-density area from defining the dose delivered to the whole breast. Fujifilm uses multiple separate AEC sensors (24 x 30 cm detector) for the calculation of the dose for the main exposure. After weightings are applied, lower AEC sensor readings are used in the calculation of the magnitude of the final exposure. This process aims to ensure that larger areas of increased density will be well penetrated but that very small high-density areas will not adversely influence the dose to the entire breast.

6.2 Filtering applied to images

Fujifilm's optical switch technology used on the Amulet FFDM systems allows the production of images with an inherently high MTF. In early software versions, including those routinely used on the original Amulet, the MTF was reduced using a pre-processing filter for achieving good balance of sharpness and noise.

With the evolution of the Amulet product to the Amulet f/s systems a second software configuration has been made available to exploit the full MTF of the system. At the time of this NHSBSP evaluation, the MTF pre-processing filter was being applied to all images acquired. With an alternate service configuration, it is now possible to assess the full MTF of the system using dedicated test menus.

REFERENCES

1. Workman A, Castellano I, Kulama E et al. *Commissioning and Routine Testing of Full Field Digital Mammography Systems* (NHSBSP Equipment Report 0604). Sheffield: NHS Cancer Screening Programmes, 2006.
2. Young KC, Johnson B, Bosmans H, et al. Development of minimum standards for image quality and dose in digital mammography. In *Digital Mammography IWDM 2004*, Proceedings of the Workshop in Durham NC, USA, June 2004, (2005).
3. Van Engen R, Young KC, Bosmans H, et al. The European protocol for the quality control of the physical and technical aspects of mammography screening. In: *European Guidelines for Quality Assurance in Breast Cancer Screening and Diagnosis*, 4th Edition, Luxembourg: European Commission, 2006.
4. Alsager A, Young KC, Oduko JM. Impact of Heel Effect and ROI Size on the Determination of Contrast-to-Noise Ratio for Digital Mammography Systems. In *Proceedings of SPIE Medical Imaging*, Bellingham WA: SPIE Publications, 2008, 69134: 1-11.
5. Young KC, Cook JJH, Oduko JM. Automated and human determination of threshold contrast for digital mammography systems. In *Proceedings of the 8th International Workshop on Digital Mammography*, Berlin: Springer-Verlag, 2006, 4046: 266-272.
6. Young KC, Alsager A, Oduko JM et al. Evaluation of software for reading images of the CDMAM test object to assess digital mammography systems. In *Proceedings of SPIE Medical Imaging*, Bellingham WA: SPIE Publications, 2008, 69131C: 1-11.
7. Young KC, Oduko JM. Technical Evaluation of Kodak DirectView Mammography Computerised Radiography System using EHR-M2 Plates (NHSBSP Equipment Report 0706). Sheffield: NHS Cancer Screening Programmes, 2007.
8. Young KC, Oduko JM. *Technical Evaluation of the Agfa CR-85 Mammography System* (NHSBSP Equipment Report 0707). Sheffield: NHS Cancer Screening Programmes, 2007.
9. Young KC, Oduko JM. *Technical Evaluation of the Hologic Selenia Full Field Digital Mammography System with a Tungsten Tube* (NHSBSP Equipment Report 0801). Sheffield: NHS Cancer Screening Programmes, 2008.
10. Young KC, Oduko JM, Gundogdu O, et al. Technical Evaluation of the GE Essential Full Field Digital Mammography System (NHSBSP Equipment Report 0803). Sheffield: NHS Cancer Screening Programmes, 2008.
11. Oduko JM, Young KC, Alsager A, et al. *Technical Evaluation of the IMS Giotto Full Field Digital Mammography System with a Tungsten Tube* (NHSBSP Equipment Report 0804). Sheffield: NHS Cancer Screening Programmes, 2008.
12. Young KC, Oduko JM, Gundogdu O et al. *Technical Evaluation of the Konica Minolta Regius 190 CR Mammography System and Three Types of Image Plate* (NHSBSP Equipment Report 0806). Sheffield: NHS Cancer Screening Programmes, 2008.

13. Young KC, Oduko JM, Gundogdu O. and Asad M. *Technical Evaluation of Profile Automatic Exposure Control Software on GE Essential Full Field Digital Mammography System* (NHSBSP Equipment Report 0903). Sheffield: NHS Cancer Screening Programmes, 2009.
14. Young KC, Oduko JM, Asad M. *Technical Evaluation of Agfa DX-M Mammography CR Reader with HM5.0 Needle-IP* (NHSBSP Equipment Report 0905). Sheffield: NHS Cancer Screening Programmes, 2009.
15. Young KC, Oduko JM, Asad M. *Technical Evaluation of Fuji Amulet Full Field Digital Mammography System* (NHSBSP Equipment Report 0907). Sheffield: NHS Cancer Screening Programmes, 2009.
16. Young KC, Oduko JM, Gundogdu O. and Alsager. *Technical Evaluation of Siemens Mammomat Inspiration Full Field Digital Mammography System* (NHSBSP Equipment Report 0909). Sheffield: NHS Cancer Screening Programmes, 2009.
17. Young KC, Oduko JM, Warren L. *Technical Evaluation of Hologic Selenia Dimensions 2-D Digital Breast Imaging System* (NHSBSP Equipment Report 1101). Sheffield: NHS Cancer Screening Programmes, 2011.